Journal of Applied Biomechanics, 2020, 36, 326-333
https://doi.org/10.1123/jab.2019-0356

Human Kinetics
COMPUTATIONAL MODEL

Contact Pressures Between the Rearfoot and a Novel Offloading Insole: Results From a Finite Element Analysis Study

Seth T. Strayer,[1] Seyed Reza M. Moghaddam,[1] Beth Gusenoff,[2] Jeffrey Gusenoff,[2] and Kurt E. Beschorner[1]

[1]University of Pittsburgh; [2]University of Pittsburgh Medical Center

Pressure offloading is critical to diabetic foot ulcer healing and prevention. A novel product has been proposed to achieve this offloading with an insole that can be easily modified for each user. This insole consists of pressurized bubbles that can be selectively perforated and depressurized to redistribute weight to the nonulcer region of the foot. However, the effect of the insole design parameters, for example, bubble height and stiffness, on offloading effectiveness is unknown. To this end, a 3-dimensional finite element model was developed to simulate contact between the rearfoot and insole. The geometry of the calcaneus bone and soft tissue was based on the medical images of an average male patient, and material properties and loading conditions based on the values reported in the literature were used. The model predicts that increasing bubble height and stiffness leads to a more effectively offloaded region. However, the model also predicts that increasing stiffness leads to increasing contact pressures on the surrounding soft tissue. Thus, a combination of insole design parameters was determined, which completely offloads the desired region, while simultaneously reducing the contact pressure on the surrounding soft tissue. This design is expected to aid in diabetic foot ulcer healing and prevention.

***Keywords**:* clinical biomechanics, footwear, modeling, rehabilitation

Diabetes mellitus is an increasingly common chronic disease that is expected to impact more than 439 million adults by the year 2030.[1] Between 10% and 15% of these patients will develop diabetic or neuropathic foot ulcers at some point during their lifetime.[2,3] One of every 6 patients with a diabetic foot ulcer will culminate in amputation in the United States. Diabetic patients with a diabetic foot ulcer, or history of ulcers, are at a heightened risk of 5- to 10-year mortality.[4] Diabetic ulcerations are costly to the patient's physical well-being and quality of life, as well as burdensome on the medical system. These ulcers typically form due to the loss of protective sensation associated with diabetes and elevated plantar pressures caused by foot deformities, gait instability, repetitive minor foot abrasions, and loss of fat pad quality. Foot pressure reduction, otherwise known as pressure offloading, is often considered the most crucial aspect of diabetic foot ulcer healing and prevention of recurrence.[3,5]

Existing treatments for pressure offloading may have significant limitations for offloading ulcers that could be addressed through innovative solutions. The total contact cast is widely accepted as the most effective offloading treatment, with up to an 87% reduction in peak pressure compared with standard, nontherapeutic footwear.[5–8] However, the total contact cast is used in fewer than 10% of ulcer cases,[9] likely due to adverse side effects, such as reduced activity level; difficulty driving, bathing, or sleeping; and the cost of treatment.[5] The removable cast boot is a safe and accessible alternative offloading device; however, these boots can be expensive, they are not customizable, and the patient's ability to remove the cast leads to problems with patient compliance.[4] Therapeutic footwear devices, such as the rocker bottom outsole and custom-made insoles, also provide some pressure relief but are considerably less effective than the total contact cast.[5] An additional option, which may achieve offloading without these side effects, is the use of insoles[10] that redistributes weight to the nonulcer region of the foot.

A novel recently developed offloading insole, PopSole™ (referred to as "insole" henceforth and whose prototype is shown in Figure 1A), consists of pressurized bubbles that can be selectively perforated and depressurized, allowing the insole to be customized based on the location, size, and severity of an ulcer. In the case of any offloading treatment, it is beneficial to assess pressures on the foot-insole couple to ensure that the device effectively offloads the desired region.[5] As a supplement to experimental data, which is often difficult and costly to obtain,[11,12] researchers have frequently utilized finite element (FE) analysis to accurately predict load distributions between the foot and its surrounding supports.[11–18] These models predict the distribution of underfoot contact pressures, given measurable design inputs, such as the geometry, material properties, and loading conditions. For example, researchers have shown that a less flexible insole material yields higher peak contact pressures on the soft tissue.[11,19] Thus, the use of FE simulations provides researchers with an opportunity for estimating the impact of insole design parameters on contact pressure distribution.

The objective of this study was to develop a 3-dimensional (3D) FE model simulating contact between the rearfoot and the insole to investigate the effects of insole design (bubble height and stiffness) on offloading effectiveness for balanced standing. It is hypothesized that (1) increased bubble height and insole stiffness will aid in preventing contact in the desired offloading region, and (2) increased stiffness will lead to increased peak contact pressures on the surrounding soft tissue.

Strayer is with the Department of Mechanical Engineering; Moghaddam and Beschorner are with the Department of Bioengineering; University of Pittsburgh, Pittsburgh, PA, USA. B. Gusenoff and J. Gusenoff are with the Department of Plastic Surgery, University of Pittsburgh Medical Center, Pittsburgh, PA, USA. Beschorner (beschorn@pitt.edu) is corresponding author.

Methods

Model Description

The FE model consisted of bone, soft tissue, and the insole (Figure 1B). The geometry of the bone and soft tissue was imported from an online computer-aided design database, which was based on the medical images of an average male patient. The geometry of the insole was constructed (design modeler add-in for ANSYS® 2019 R1; ANSYS Inc, Canonsburg, PA) after geometry cleaning and smoothing was performed using Geomagic® (3D Systems, Rock Hill, SC). The base plate of the insole had constant dimensions of 9 cm (length or x), 8.5 cm (width or z), and 0.2 cm (height or y), and a total loading area (designated by the exterior of the bubble region) of 66 cm^2. The offloading area (where the bubbles are popped in the center of the base plate) was kept constant at 5.6 cm^2. Although the size of ulcers can vary (0–20 cm^2),[20,21] the median size of ulcers (~1 cm^2)[20,22] is smaller than this offloading area. Thus, the simulated offloading region should accommodate the majority of ulcers. Previous research shows that, for balanced standing, peak pressures are in the rearfoot region.[11,12] Hence, to minimize computational expense, only the rearfoot was included in this model. The location of the offloading area was chosen as the heel since it is among the most common locations for

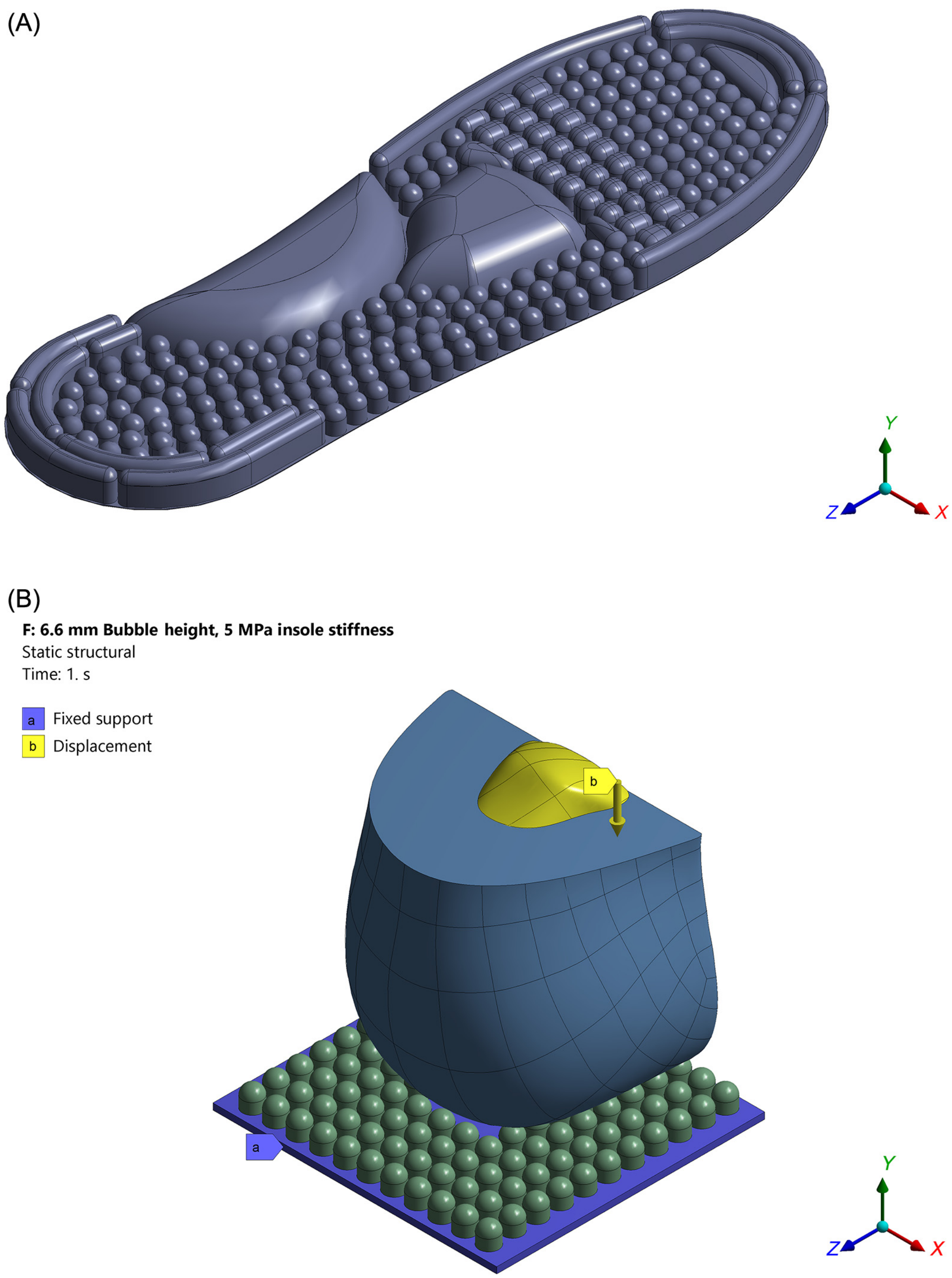

Figure 1 — (A) Prototype PopSole™ geometry. (B) Finite element model with prescribed boundary conditions.

Table 1 Material Properties of the Bone and Insole Components

Component	Young modulus, E (MPa)	Poisson ratio, ν
Bone	7300	0.3
Insole	3, 5, 10	0.4

Table 2 Coefficients of the Hyperelastic Material Model Used to Simulate the Soft Tissue

C_{10}	C_{01}	C_{20}	C_{11}	C_{02}	D_1	D_2
85,550	−58,400	38,920	−23,100	8484	0.4370E-05	0.6811E-06

Note: Units are Pa for C_{ij} and Pa^{-1} for D_i.

ulcers[23] and contains a large area for redistributing loads compared with other regions of the foot (eg, the hallux). Thus, ulcers in the heel are considered a viable candidate for this type of insole. The model was then imported and assembled in ANSYS® Workbench.

The bone and insole components were modeled using linear elastic, homogenous, and isotropic material properties (Table 1). The soft tissue was modeled as a nonlinear elastic material based on stress–strain data adopted from *in vivo* ultrasonic measurements.[17] The hyperelastic material model (ANSYS®) was chosen to represent the nonlinear and nearly incompressible nature of the soft tissue and its strain-hardening characteristic.[24] The second-order polynomial strain energy potential was chosen to represent this model and is given by Equation 1,

$$U = \sum\nolimits_{i+j=1}^{2} C_{ij}(\bar{I}_1 - 3)^i(\bar{I}_2 - 3)^j + \sum\nolimits_{i=1}^{2} \frac{1}{D_i}(J_{\mathrm{el}} - 1)^{2i} \quad (1)$$

where U (in Pa) is the strain energy density and $\bar{I}_1$, $\bar{I}_2$, and J_{el} (dimensionless) are the first and second deviatoric strain invariants and elastic volume ratio, respectively. The coefficients C_{ij} (in Pa) and D_i (in Pa^{-1}) are the coefficients of the hyperelastic material model (Table 2).[12,17] Although patients with diabetes mellitus or peripheral neuropathy tend to have stiffer plantar soft tissue than their healthy counterparts,[15,25,26] this effect is small in the heel region.[26] Thus, using material properties from healthy adults is appropriate for this model. The Young modulus and Poisson ratio of the bone were assigned as 7300 MPa and 0.3, respectively, based on the formulation developed by Nakamura et al[18] and used in analyses henceforth.[12,13,15,16] The Young modulus of the insole was varied at 3, 5, and 10 MPa to investigate the effect of insole stiffness on offloading effectiveness. These values are within the soft regime for the PVC material from which the insole is manufactured. This regime was determined based on the range of the Young modulus for common insole materials.[11] The Poisson ratio (Table 1) was chosen based on the existing literature.[11,12]

The foot-insole contact couple was modeled using an augmented Lagrange frictional contact formulation. It is a penalty-based method that employs a nondimensional stiffness factor between contacting bodies, which helps prevent penetration. Therefore, this approach minimized penetration in the foot-insole contact region and helped ensure convergence.[24] A friction coefficient of 0.6 was chosen based on existing literature.[11,12,27]

Displacement boundary conditions were applied to the base plate of the insole and the top surface of the bone. The base plate of the insole was assigned a zero-displacement boundary condition, simulating fixed support. The top surface of the bone was displaced downward (ie, in the negative y-direction, toward the insole), while the x- and z-directions were assigned zero displacement (Figure 1B). The magnitude of this displacement was iteratively controlled to achieve the desired vertical reaction force on the support (ie, the base plate of the insole).[28] A reaction force of 130 N was generated for all analyses (see the "Parametric Analysis" section for rationale). Using displacement boundary conditions improved the stability of the solution compared with using applied force boundary conditions. Both the base plate of the insole and the top surface of the bone were assigned zero-rotation boundary conditions, that is, they were not free to rotate.

Mesh Considerations

The mesh of the FE model was assigned in a bias fashion, that is, the mesh was more refined in those areas that were expected to be in contact. Body and face sizing methods (ANSYS®) were used to produce the refined mesh. The patch conforming tetrahedron method was applied to the insole, given its complex geometry.[29] Mesh convergence studies were performed (see the "Verification and Validation" section) in which the mesh was refined until there was less than a 5% change in the peak contact pressure on the surrounding soft tissue (Table 3) for 2 consecutive reductions in mesh size. The refined mesh state for any model used a minimum mesh size of 1.5 mm, leading to upwards of 100,000 quadratic, tetrahedral elements (Figure 2, Table 3).

Verification and Validation

Verification and validation studies[30] were conducted to assess the stability and accuracy of the current model. Contact between the rearfoot and a 5-mm thick flat plate with Young modulus of 17,000 MPa was simulated for these studies.[12] First, verification was performed using this model until 2 consecutive mesh refinements yielded less than a 5% change in peak contact pressure on the rearfoot soft tissue (Table 3). Once verification was achieved at the mesh size of 1.5 mm, cross-validation of the FE model was performed by comparing the verified, computed peak contact pressure on the rearfoot soft tissue with the value from the literature (0.23 MPa). Given the accuracy of the Cheung et al[12] model with experimental results, this was considered an appropriate benchmark for validating the current model. The refined mesh state yielded a ~1% error when compared with the peak contact pressure from the literature. Thus, the proposed model, using the specified contact formulation and boundary conditions as outlined in "Model Description" section, achieved cross-validation regarding peak contact pressure on the rearfoot soft tissue when compared with the values from the literature.

Parametric Analysis

A total of 12 different simulations were conducted to investigate the effects that bubble height and insole stiffness have on offloading effectiveness. All simulations in this study were performed to achieve the desired reaction force of 130 N. This force was calculated based on the weight applied by a person with a body mass of ~70 kg on only the rearfoot region of the foot (~350 N per foot · 0.37). The proportion of weight on the rearfoot (0.37) was estimated based on the ratio of the contact area in this region.[12] Models using partial loading for partial-foot models[31,32] have been employed based on the estimation of load applied to only those partial regions.[33] During postprocessing, we considered 2 specific contact regions: (1) the contact between the soft tissue and the nonpopped bubbles and (2) between the soft tissue and the support

Table 3 Verification of the Flat Plate Cross-Validation Model

Mesh size, mm	Number of elements	Peak contact pressure, MPa
5.0	1.4×10^4	0.20
3.0	2.8×10^4	0.20
2.0	6.7×10^4	0.23
1.5	1.4×10^5	0.23

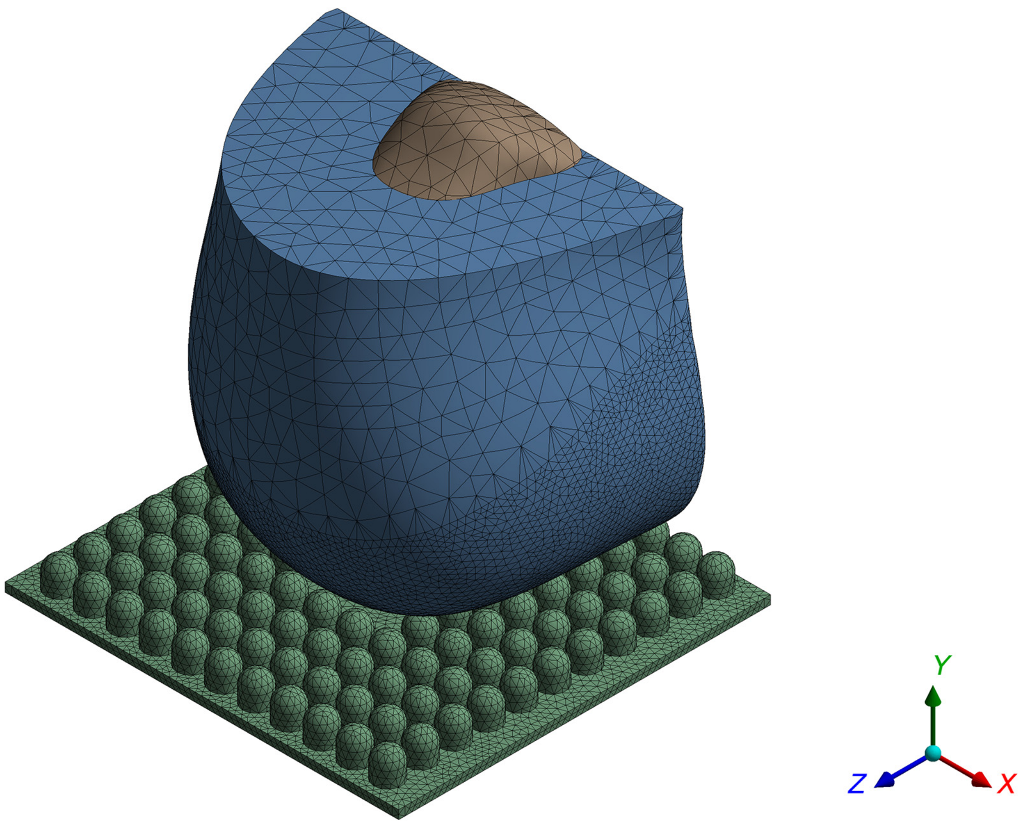

Figure 2 — Refined mesh state of the finite element model.

(ie, the popped-bubble region). The former describes the pressure in the soft tissue surrounding the offloading region. The latter describes the pressure in the offloading region.

Results

Contour plots were constructed to depict the predicted peak contact pressure for the surrounding soft tissue (Figure 3A) and the desired offloading region (Figure 3B) as functions of the insole bubble height (h) and Young modulus (E). The range of predicted peak contact pressures on the surrounding soft tissue was 290 to 660 kPa for a bubble height of 4.9 mm, 280 to 520 kPa for a height of 6.6 mm, 300 to 520 kPa for a height of 8.3 mm, and 250 to 520 kPa for a height of 10 mm. The range of predicted peak contact pressures on the offloaded region was 79 to 92 kPa for a bubble height of 4.9 mm and 38 to 48 kPa for a bubble height of 6.6 mm. Except for a bubble height of 8.3 mm and insole stiffness of 3 MPa, all other combinations of bubble height and insole stiffness completely offloaded the region, yielding 0 contact pressures (Figure 3B). A bubble height of 8.3 mm and insole stiffness of 5 MPa fully offloaded the area (Figure 3B) while simultaneously minimizing the pressure on the surrounding soft tissue (Figure 3A). The peak contact pressure on the surrounding soft tissue was 390 kPa for this case.

The qualitative effect that bubble height and insole stiffness have on offloading effectiveness is demonstrated in Figure 4A and 4B. For a fixed height of 8.3 mm, the flexible material ($E = 3$ MPa) leads to foot-insole contact in the offloading region (Figure 4A, the foot is contacting the insole), whereas the stiffer material ($E = 5$ MPa) prevents contact (Figure 4B, there is no foot-insole contact).

Figure 5 depicts the contact pressure distribution on the surrounding soft tissue at the bubble height of 8.3 mm and insole stiffness of 5 MPa. As stated, this combination fully offloaded the area, yielding 0 contact pressures (and subsequently 0 contact area) in that region. Where the bubbles are in contact with the soft tissue, the maximum pressure is 390 kPa in the tissue closest to the offloaded region. In this case, the contact area, which was extracted during postprocessing using ANSYS Parametric Design Language (APDL) command-line arguments, was 9.2 cm^2, yielding an average analytical contact pressure of $\sigma_{\text{ave}} = 140$ kPa.

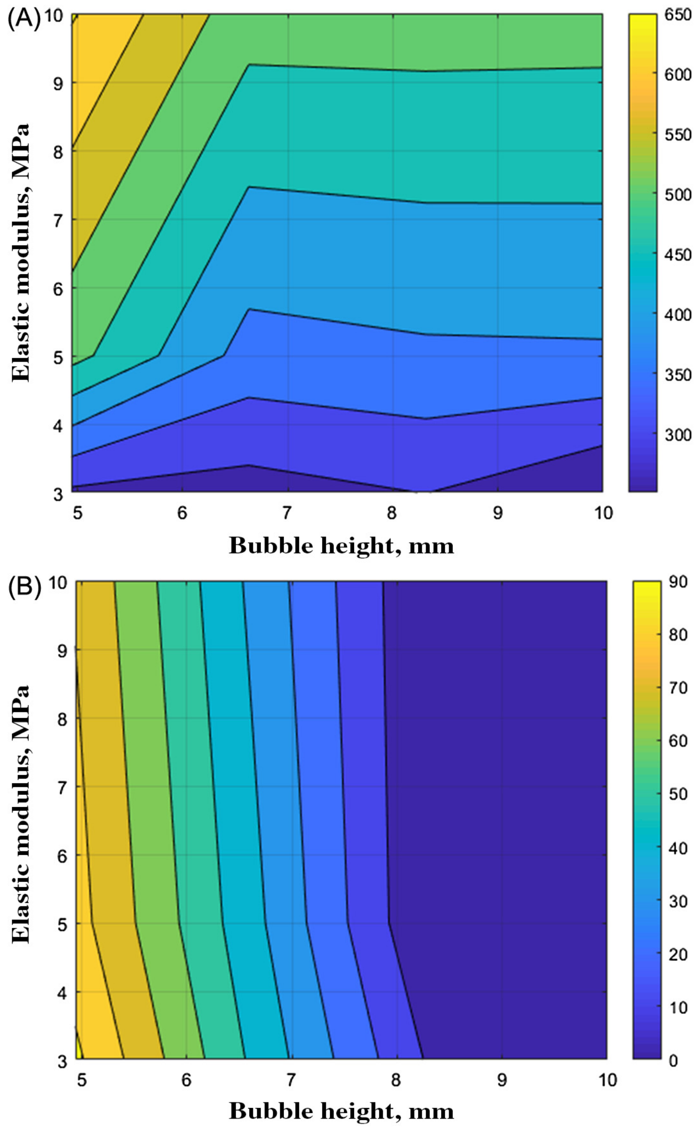

Figure 3 — Predicted peak contact pressure (in kPa) on (A) the surrounding soft tissue and (B) the offloading region for varying values of h, E. E indicates Young modulus; h, insole bubble height.

Discussion

In this study, a 3D FE model simulating contact between the rearfoot and the insole was developed to investigate the effects of insole design (bubble height and stiffness) on offloading effectiveness for balanced standing. It was hypothesized that (1) increased bubble height and insole stiffness will aid in preventing contact in the desired offloading region and (2) increased stiffness will lead to increased peak contact pressures on the surrounding soft tissue. Indeed, the model predicts that increases in bubble height and insole stiffness lead to reduced contact pressures in the offloaded region and that increased insole stiffness leads to increased contact pressures on the surrounding soft tissue. Thus, a combination of insole design parameters that completely offload the region, while simultaneously minimizing contact pressure on the surrounding soft tissue, should be considered.

The authors acknowledge some limitations of the current study. First, the applied vertical displacement (force) was selected to reflect balanced standing. Larger forces are expected during gait or for higher-weight individuals. While comparable trends would be expected for gait, the optimal working conditions of the insole may be different in the presence of dynamic or higher loads. Another limitation is that the FE solutions did not converge with further mesh refinement for 2 insole design parameter sets (a bubble height of 8.3 and 10 mm with a Young modulus of 3 MPa). We suspect that this was due to the buckling of the bubble "columns" caused by the combination of increased height and low stiffness. Also, stiffer plantar soft tissue, a direct result of diabetes mellitus and peripheral neuropathy,[15,25,26] was not modeled in the current study. While this factor would lead to increased stresses in the local region, it is not expected to change the overall data trends regarding the insole design parameters. Finally, the authors acknowledge the lack of experimental validation for study-specific analyses.

The simulations predict that increased bubble height and insole stiffness lead to a more effectively offloaded region. The minimum bubble height needed to prevent foot-insole contact was determined to be 8.3 mm. For any heights lower than this, the simulations predict a concentration of contact pressures in the offloading region, regardless of the insole stiffness. Furthermore, at the height of 8.3 mm, an insole stiffness value of at least 5 MPa was necessary to prevent foot-insole contact. For the combination of insole design parameters that completely prevents contact (8.3 mm bubble height and 5 MPa insole stiffness), any additional increase in those parameters will not yield an additional benefit in terms of offloading the desired region (ie, increasing the bubble height and insole stiffness to 10 mm and 10 MPa, respectively, had no further effect on the offloading effectiveness). In further consideration, increasing the insole stiffness to 10 MPa will lead to a significant increase in peak contact pressures in the surrounding soft tissue, which may cause pain and the development of new ulcers.[12] Hence, from the FE predictions, this combination of design parameters represents the optimal working condition of the insole for balanced standing (ie, this combination completely offloads the desired region while simultaneously minimizing pressure on the surrounding soft tissue).

The benefits of offloading a specific region of the foot should be weighed against a potential increase in contact pressures on the surrounding soft tissue due to the reduction of the loaded area. That is, there is a trade-off: contact pressure in the offloading area may be 0, but increased contact pressures in the surrounding soft tissue may cause pain and the development of new ulcers.[12] Clinically, it is important to evaluate the trade-off between offloading the ulcer region to promote healing while considering the potential for new ulcer development in the region adjacent to the offloading.

Although the insole stiffness provides significant contributions to the magnitude of peak contact pressures in the surrounding soft tissue, the simulations predict that bubble height alone is negligible in determining the peak contact pressure on the surrounding soft tissue. Specifically, the results indicate that peak contact pressure on the surrounding soft tissue was insensitive to bubble height. For example, for heights of 6.6 and 10 mm, at a stiffness of 10 MPa, the calculated peak pressures on the surrounding soft tissue differed by less than 1% (Figure 3A). These results indicate that the alteration of bubble height mainly influences contact pressures on the offloading region and not on the surrounding soft tissue. Thus, increasing bubble height should only be done to provide better offloading effects.

The results of this study were found to be consistent with previous studies that have simulated the effect of insole stiffness on peak contact pressures on the foot.[11,19] In agreement with these

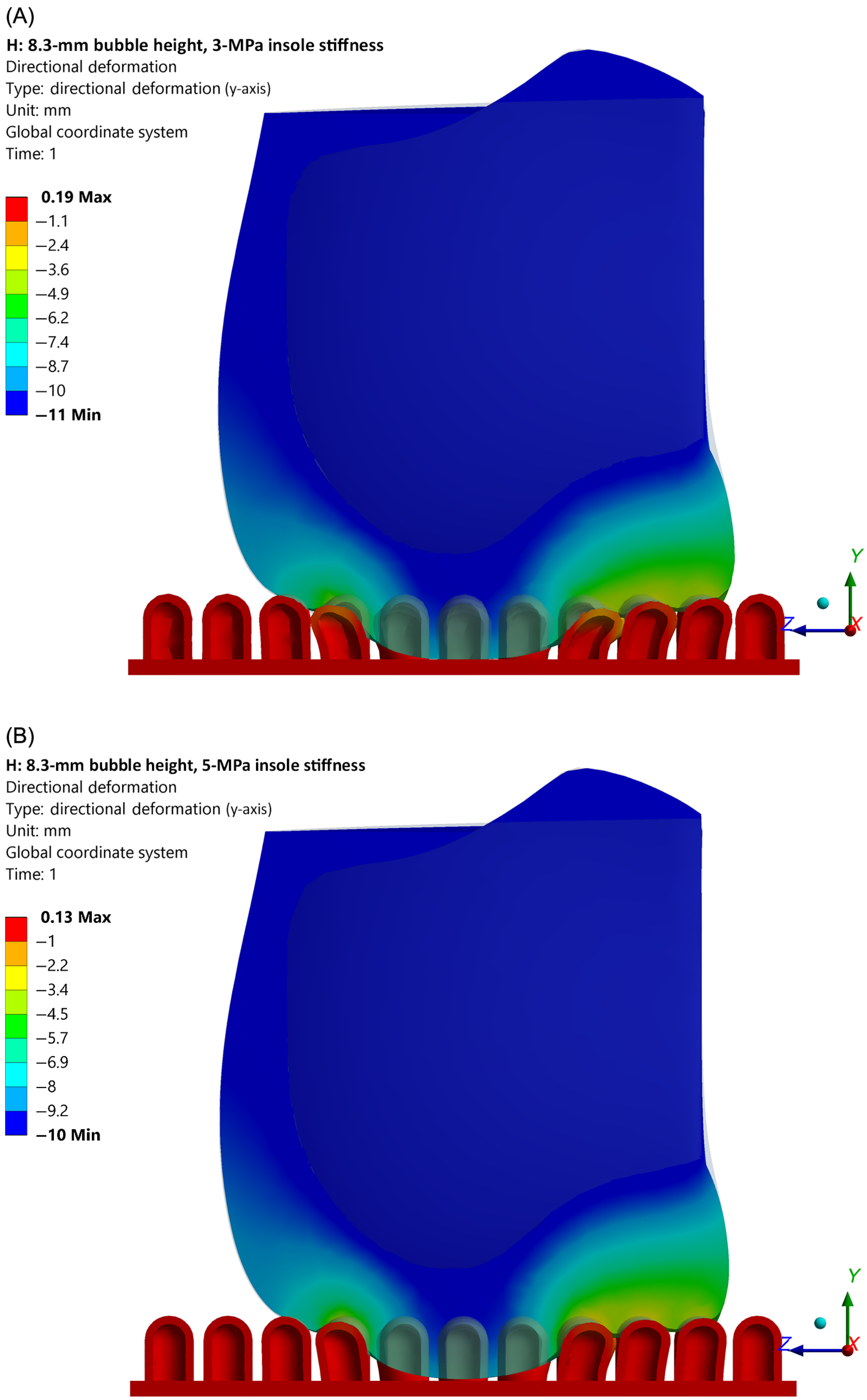

Figure 4 — Section demonstrating offloading effectiveness for $h = 8.3$ mm and (A) $E = 3$ MPa, (B) $E = 5$ MPa. In (A), the foot is contacting the support. In (B), there is no contact. E indicates Young modulus; h, insole bubble height.

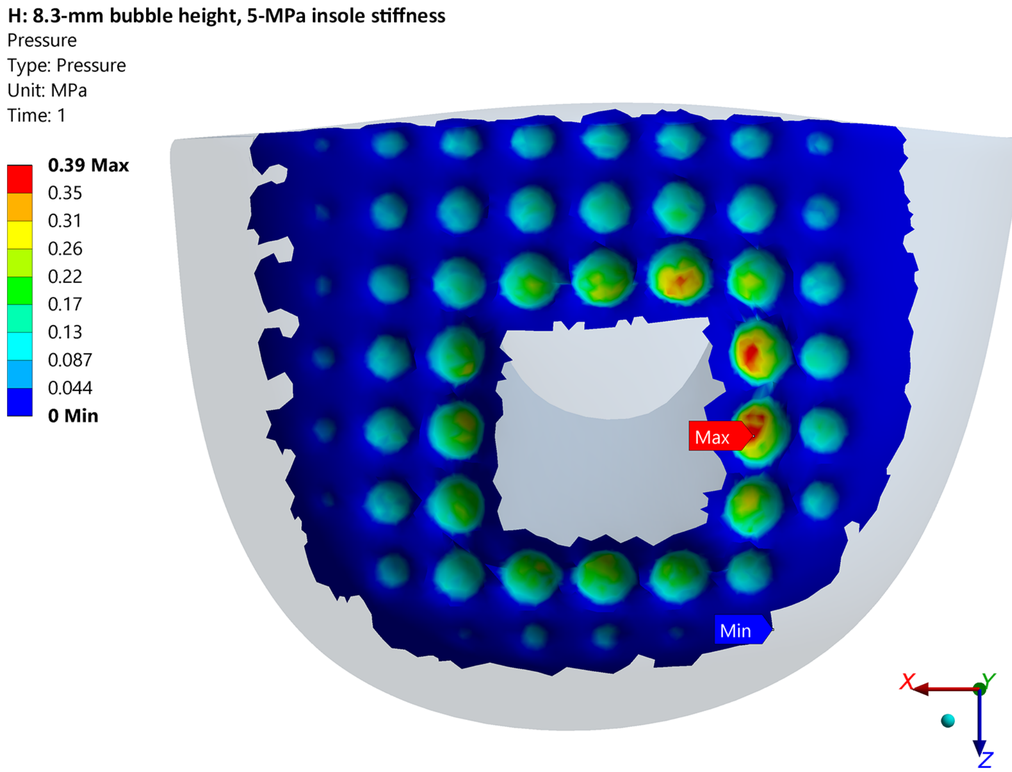

Figure 5 — Contact pressure distribution on the surrounding soft tissue for h = 8.3 mm and $E = 5$ MPa. E indicates Young modulus; h, insole bubble height.

studies, the FE model predicts that increased insole stiffness leads to increased peak contact pressure on the soft tissue. Also, the FE model achieved similar (~1% error) peak contact pressures in the cross-validation study.[12] Regarding the results of the offloading insole, we do not expect peak contact pressures to be comparable to those predicted in Cheung et al,[12] due to the geometry of the insole, which generates a stress profile consistent with Hertzian point contact.[34]

The results from this study are expected to help aid in the design of the insole for offloading the desired region of diabetic foot ulcers. In particular, this model can be considered a preliminary step in the determination of insole design parameters, which most effectively offload the desired region for persons of different weight or stature. This can provide significant benefits in diabetic foot ulcer healing and prevention of recurrence.[3,5] Based on the success of the cross-validation study,[12] the convergence of the model with existing trends in the literature,[11,19] and the confirmation of our original hypothesis, the authors are confident in the accuracy and stability of the current model.

An accurate, yet simplified, 3D FE model of the rearfoot and insole was developed to investigate the effects of offloading insole design parameters (bubble height and stiffness) on offloading effectiveness. The FE simulations predict that the offloading insole can completely mitigate pressure in a desired offloading region under certain combinations of these parameters. In general, increasing bubble height and insole stiffness reduces contact pressures in the offloading region; however, increasing stiffness also leads to increasing contact pressures on the surrounding soft tissue. Thus, an optimal combination of insole design parameters was determined, one that completely offloads the desired region while simultaneously minimizing peak contact pressures on the surrounding soft tissue. The best parameters for balanced standing were a bubble height of 8.3 mm and an insole stiffness of 5 MPa.

Acknowledgments

This projected was supported by the Center for Medical Innovation at the University of Pittsburgh (F 228-2018). The authors have no conflicts of interest to disclose.

References

1. Shaw JE, Sicree RA, Zimmet PZ. Global estimates of the prevalence of diabetes for 2010 and 2030. *Diabetes Res Clin Pract*. 2010;87(1):4–14. PubMed ID: 19896746 doi:10.1016/j.diabres.2009.10.007
2. Margolis DJ, Malay DS, Hoffstad OJ, et al. Prevalence of diabetes, diabetic foot ulcer, and lower extremity amputation among Medicare beneficiaries, 2006 to 2008. In Data Points Publication Series [Internet]. 2011, Feb 11. Agency for Healthcare Research and Quality (US). AHRQ Publication No. 10(11)-EHC009-EF.
3. Yazdanpanah L, Nasiri M, Adarvishi S. Literature review on the management of diabetic foot ulcer. *World J Diabetes*. 2015;6(1):37. PubMed ID: 25685277 doi:10.4239/wjd.v6.i1.37
4. Boulton AJ, Armstrong DG, Kirsner RS, et al. Diagnosis and management of diabetic foot complications. *American Diabetes Association*. 2018.
5. Bus SA. The role of pressure offloading on diabetic foot ulcer healing and prevention of recurrence. *Plast Reconstr Surg*. 2016;138(3S):179S–187S. doi:10.1097/PRS.0000000000002686
6. Bus SA, Van Deursen R, Armstrong D, et al. Footwear and offloading interventions to prevent and heal foot ulcers and reduce plantar

pressure in patients with diabetes: a systematic review. *Diabetes Metab Res Rev*. 2016;32(Suppl. 1):99–118. PubMed ID: 26342178 doi:10.1002/dmrr.2702
7. Cavanagh PR, Bus SA. Off-loading the diabetic foot for ulcer prevention and healing. *Plast Reconstr Surg*. 2011;127(Suppl. 1):248S–256S. PubMed ID: 21200298 doi:10.1097/PRS.0b013e3182024864
8. Fleischli JG, Lavery LA, Vela SA, Ashry H, Lavery DC. 1997 William J. Stickel Bronze Award. Comparison of strategies for reducing pressure at the site of neuropathic ulcers. *J Am Podiatr Med Assoc*. 1997;87(10):466–472. PubMed ID: 9351316 doi:10.7547/87507315-87-10-466
9. Fife CE, Carter MJ, Walker D. Why is it so hard to do the right thing in wound care? *Wound Repair Regen*. 2010;18(2):154–158. PubMed ID: 20163568 doi:10.1111/j.1524-475X.2010.00571.x
10. Bus SA, Ulbrecht JS, Cavanagh PR. Pressure relief and load redistribution by custom-made insoles in diabetic patients with neuropathy and foot deformity. *Clin Biomech*. 2004;19(6):629–638. doi:10.1016/j.clinbiomech.2004.02.010
11. Cheung JT-M, Zhang M. A 3-dimensional finite element model of the human foot and ankle for insole design. *Arch Phys Med Rehabil*. 2005;86(2):353–358. PubMed ID: 15706568 doi:10.1016/j.apmr.2004.03.031
12. Cheung JT-M, Zhang M, Leung AK-L, Fan Y-B. Three-dimensional finite element analysis of the foot during standing—a material sensitivity study. *J Biomech*. 2005;38(5):1045–1054. PubMed ID: 15797586 doi:10.1016/j.jbiomech.2004.05.035
13. Chen W-M, Lee S-J, Lee PVS. Plantar pressure relief under the metatarsal heads–therapeutic insole design using three-dimensional finite element model of the foot. *J Biomech*. 2015;48(4):659–665. PubMed ID: 25620685 doi:10.1016/j.jbiomech.2014.12.043
14. Chen W-P, Ju C-W, Tang F-T. Effects of total contact insoles on the plantar stress redistribution: a finite element analysis. *Clin Biomech*. 2003;18(6):S17–S24. doi:10.1016/S0268-0033(03)00080-9
15. Gefen A. Plantar soft tissue loading under the medial metatarsals in the standing diabetic foot. *Med Eng Phys*. 2003;25(6):491–499. PubMed ID: 12787987 doi:10.1016/S1350-4533(03)00029-8
16. Gefen A, Megido-Ravid M, Itzchak Y, Arcan M. Biomechanical analysis of the three-dimensional foot structure during gait: a basic tool for clinical applications. *J Biomech Eng*. 2000;122(6):630–639. PubMed ID: 11192385 doi:10.1115/1.1318904
17. Lemmon D, Shiang T-Y, Hashmi A, Ulbrecht JS, Cavanagh PR. The effect of insoles in therapeutic footwear—a finite element approach. *J Biomech*. 1997;30(6):615–620. PubMed ID: 9165395 doi:10.1016/S0021-9290(97)00006-7
18. Nakamura S, Crowninshield R, Cooper R. An analysis of soft tissue loading in the foot–a preliminary report. *Bull Prosthet Res*. 1981;10:27–34. PubMed ID: 7332829
19. Goske S, Erdemir A, Petre M, Budhabhatti S, Cavanagh PR. Reduction of plantar heel pressures: Insole design using finite element analysis. *J Biomech*. 2006;39(13):2363–2370. PubMed ID: 16197952 doi:10.1016/j.jbiomech.2005.08.006
20. Oyibo S, Jude E, Tarawneh I, et al. The effects of ulcer size and site, patient's age, sex and type and duration of diabetes on the outcome of diabetic foot ulcers. *Diabet Med*. 2001;18(2):133–138. PubMed ID: 11251677 doi:10.1046/j.1464-5491.2001.00422.x
21. Zimny S, Schatz H, Pfohl M. The effects of ulcer size on the wound radius reductions and healing times in neuropathic diabetic foot ulcers. *Exp Clin Endocrinol Diabetes*. 2004;112(04):191–194. doi:10.1055/s-2004-817932
22. Beckert S, Witte M, Wicke C, Königsrainer A, Coerper S. A new wound-based severity score for diabetic foot ulcers: a prospective analysis of 1,000 patients. *Diabetes Care*. 2006;29(5):988–992. PubMed ID: 16644625 doi:10.2337/dc05-2431
23. Cowley MS, Boyko EJ, Shofer JB, Ahroni JH, Ledoux WR. Foot ulcer risk and location in relation to prospective clinical assessment of foot shape and mobility among persons with diabetes. *Diabetes Res Clin Pract*. 2008;82(2):226–232. PubMed ID: 18829126 doi:10.1016/j.diabres.2008.07.025
24. Bhashyam GR. ANSYS mechanical, a powerful nonlinear simulation tool. *Ansys, Inc*. 2002;1(1):39.
25. Gefen A, Megido-Ravid M, Azariah M, Itzchak Y, Arcan M. Integration of plantar soft tissue stiffness measurements in routine MRI of the diabetic foot. *Clin Biomech*. 2001;16(10):921–925. doi:10.1016/S0268-0033(01)00074-2
26. Klaesner JW, Hastings MK, Zou D, Lewis C, Mueller MJ. Plantar tissue stiffness in patients with diabetes mellitus and peripheral neuropathy. *Arch Phys Med Rehabil*. 2002;83(12):1796–1801. PubMed ID: 12474190 doi:10.1053/apmr.2002.35661
27. Zhang M, Mak A. In vivo friction properties of human skin. *Prosthet Orthot Int*. 1999;23(2):135–141. PubMed ID: 10493141 doi:10.3109/03093649909071625
28. Mirhassani Moghaddam SR. *Computational Models for Predicting Shoe Friction and Wear*. [Doctoral Dissertation]. Pittsburgh, PA: University of Pittsburgh; 2018.
29. Ansys Inc. *ANSYS Meshing User's Guide*. Canonsburg, PA: Ansys, Inc.; 2010; 15317:724–746.
30. ASME Standard V&V 40. *Assessing Credibility of Computational Modeling Through Verification and Validation: Application to Medical Devices*. New York, NY; 2018.
31. Wu L. Nonlinear finite element analysis for musculoskeletal biomechanics of medial and lateral plantar longitudinal arch of virtual Chinese human after plantar ligamentous structure failures. *Clin Biomech*. 2007;22(2):221–229. doi:10.1016/j.clinbiomech.2006.09.009
32. Wu L, Zhong S, Zheng R, et al. Clinical significance of musculoskeletal finite element model of the second and the fifth foot ray with metatarsal cavities and calcaneal sinus. *Surg Radiol Anat*. 2007;29(7):561–567. PubMed ID: 17619812 doi:10.1007/s00276-007-0231-3
33. Simkin A. *Structural Analysis of the Human Foot in Standing Posture*. [Dissertation]. Tel Aviv, Israel: Tel Aviv University; 1982.
34. Johnson KL, Johnson KL. *Contact Mechanics*. Cambridge, United Kingdom: Cambridge University Press; 1987.